Molecular Biology of the Cell
Vol. 12, 367–381, February 2001

# A Di-Leucine Sequence and a Cluster of Acidic Amino Acids Are Required for Dynamic Retention in the Endosomal Recycling Compartment of Fibroblasts

**Amy O. Johnson, Michael A. Lampson, and Timothy E. McGraw***

Department of Biochemistry, Weill Graduate School of Medical Sciences of Cornell University, New York, New York 10021

Submitted July 18, 2000; Revised November 13, 2000; Accepted November 16, 2000
Monitoring Editor: Juan Bonifacino

Insulin-regulated aminopeptidase (IRAP), a transmembrane aminopeptidase, is dynamically retained within the endosomal compartment of fibroblasts. The characteristics of this dynamic retention are rapid internalization from the plasma membrane and slow recycling back to the cell surface. These specialized trafficking kinetics result in <15% of IRAP on the cell surface at steady state, compared with 35% of the transferrin receptor, another transmembrane protein that traffics between endosomes and the cell surface. Here we demonstrate that a 29-amino acid region of IRAP's cytoplasmic domain (residues 56–84) is necessary and sufficient to promote trafficking characteristic of IRAP. A di-leucine sequence and a cluster of acidic amino acids within this region are essential elements of the motif that slows IRAP recycling. Rapid internalization requires any two of three distinct motifs: M[15,16], DED[64–66], and LL[76,77]. The DED and LL sequences are part of the motif that regulates recycling, demonstrating that this motif is bifunctional. In this study we used horseradish peroxidase quenching of fluorescence to demonstrate that IRAP is dynamically retained within the transferrin receptor-containing general endosomal recycling compartment. Therefore, our data demonstrate that motifs similar to those that determine targeting among distinct membrane compartments can also regulate the rate of transport of proteins from endosomal compartments. We propose a model for dynamic retention in which IRAP is transported from the general endosomal recycling compartment in specialized, slowly budding recycling vesicles that are distinct from those that mediate rapid recycling back to the surface (e.g., transferrin receptor-containing transport vesicles). It is likely that the dynamic retention of IRAP is an example of a general mechanism for regulating the distribution of proteins between the surface and interior of cells.

## INTRODUCTION

Segregation of proteins and lipids into the discrete organelles of the secretory and endocytic pathways is fundamental to cell structure and function. This heterogeneity is established and maintained despite continuous and extensive membrane flow through the biosynthetic and endocytic pathways. To preserve their biochemical identity, these compartments must efficiently sort and remove nonresident proteins and lipids while ensuring the retention of resident molecules (Rothman and Wieland, 1996).

One mechanism for retention of proteins in organelles is to prevent their inclusion in transport vesicles that bud from a compartment. This mechanism can be thought of as a "static" retention process in which resident proteins are physically prevented from leaving a compartment (for reviews see Nilsson *et al.*, 1991; Swift and Machamer, 1991). Inhibition of transport from a compartment can be achieved by tethering proteins to the cytoskeleton, formation of protein aggregates that are too large to enter transport vesicles, localization to membrane microdomains that restrict packaging into transport vesicles, or concentration of proteins into vesicles that slowly bud from the compartment (Nilsson *et al.*, 1991; Swift and Machamer, 1991; Mays *et al.*, 1995; Liu *et al.*, 1997; Simons and Ikonen, 1997; Sutterlin *et al.*, 1997; Keller and Simons, 1998). The selective retrieval of proteins that have escaped from an organelle also plays a key role in

* Corresponding author. E-mail address: temcgraw@mail.med.cornell.edu.

Abbreviations used: CHO, Chinese Hamster ovary; DAB, diaminobenzidine; ERC, endosomal recycling compartment; FBS, fetal bovine serum; F-WGA, fluorescein wheat germ agglutinin; HRP, horseradish peroxidase; IRAP, insulin-regulated aminopeptidase; Tf, transferrin; TR, transferrin receptor; TGN, trans-Golgi network.

the localization of proteins to specific membrane compartments (Bryant and Stevens, 1997; Cosson *et al.*, 1998; Ghosh *et al.*, 1998; Andersson *et al.*, 1999; Eng *et al.*, 1999; Mallet and Maxfield, 1999). These two mechanisms for localization are not incompatible. In many cases the steady-state localization of a protein within a compartment is dynamic, achieved by slow transport from the compartment coupled with rapid retrieval back to the compartment (e.g., Bryant and Stevens, 1997; Liu *et al.*, 1997; Andersson *et al.*, 1999). Two examples of proteins that are dynamically retained within an organelle are TGN38 and furin. Both of these proteins continually cycle between the plasma membrane, endosomes, and the TGN, and the kinetics of their trafficking are such that at steady state these proteins are highly concentrated in the TGN (Jones *et al.*, 1995; Schafer *et al.*, 1995; Takahashi *et al.*, 1995; Ghosh *et al.*, 1998; Mallet and Maxfield, 1999).

Previous studies have shown that the efficient retrieval of proteins is mediated by motifs that mediate selective concentration in vesicles destined for transport back to the resident compartment (Jackson *et al.*, 1990; Trowbridge *et al.*, 1993; Takahashi *et al.*, 1995; Bryant and Stevens, 1997; Cosson *et al.*, 1998). The motifs that target proteins to various intracellular transport vesicles are similar to those motifs that mediate rapid internalization from the plasma membrane. Less molecular detail is known about the motifs that slow the transport of specific proteins from a compartment.

Protein localization along the biosynthetic pathway has been extensively studied, whereas less is known about the mechanism for retention of proteins within the endocytic pathway. Recent evidence suggests that some proteins are dynamically retained within the endosomal system (Johnson *et al.*, 1993; Mayor *et al.*, 1993, 1994; Marsh *et al.*, 1995b). For example, GPI-linked proteins are dynamically concentrated in the endosomal recycling compartment (ERC), relative to many of the transmembrane proteins that rapidly traffic through this compartment, based on slow transport from the ERC coupled with efficient retrieval from the plasma membrane (Mayor *et al.*, 1998). We have recently shown that the pericentriolar ERC of Chinese hamster ovary (CHO) cells is capable of dynamically retaining transmembrane proteins as well (Johnson *et al.*, 1998). In those studies we used a chimera, vpTR, in which the cytoplasmic domain of the IRAP aminopeptidase is coupled to the transmembrane and extracellular domains of the human transferrin (Tf) receptor (TR). VpTR, a surrogate for IRAP trafficking, is dynamically retained within the ERC (Johnson *et al.*, 1998). vpTR is transported from this compartment at one-third the rate of the TR and it is internalized from the cell surface as rapidly as is the TR. Consequently, at steady state <15% of vpTR is on the surface compared with 35% of the TR on the cell surface.

IRAP is a major component of GLUT4-containing vesicles isolated from fat cells (Kandror and Pilch, 1994; Kandror *et al.*, 1994; Keller *et al.*, 1995). GLUT4, the "insulin-regulated" glucose transporter isoform, is highly expressed in fat and muscle, whereas IRAP is expressed in a variety of cell types, including CHO cells (Keller *et al.*, 1995; Johnson *et al.*, 1998). In fat and muscle, the kinetics of GLUT4 and IRAP trafficking are similar, and to date, IRAP is the only protein known to traffic like GLUT4 (Ross *et al.*, 1996, 1997). These data indicate that IRAP and GLUT4 are both trafficked by the same specialized insulin-regulated pathway in fat and muscle cells. The physiological function of IRAP is not known, and it is unclear why it is concentrated in GLUT4-containing vesicles in fat and muscle or why it is dynamically retained within endosomes of fibroblasts. In this regard, it is of interest to note that vpTR is translocated to the cell surface of fibroblasts after insulin treatment, demonstrating that in these cells the dynamic retention of IRAP is reversible. Translocation of IRAP to the cell surface may regulate IRAP function by exposing its extracellular domain, which contains the aminopeptidase activity, to potential extracellular substrates.

Morphological methods are commonly used in studies of the motifs that target proteins to specialized endocytic trafficking pathways that are physically distinct from the general endosomal recycling system (e.g., Ghosh *et al.*, 1998; Xiang *et al.*, 2000). Morphological methods cannot be used to identify the motifs that regulate IRAP trafficking because the dynamic retention pathway is kinetically distinct but morphologically identical to the constitutive endosomal recycling pathway (Johnson *et al.*, 1998). The advantage of using vpTR as a reporter for studies of the dynamic retention mechanism is that the kinetics of the individual transport steps that determine the steady-state distribution of vpTR can be measured. In this report we exploit this advantage in an analysis of the motifs that determine the kinetics of IRAP traffic. We find that a 29-amino acid region of IRAP's cytoplasmic domain is necessary and sufficient for dynamic retention within endosomes. We show that a cluster of acidic amino acids in conjunction with the previously identified di-leucine sequence are essential elements of the dynamic retention motif. This cluster of acidic amino acids/di-leucine motif is bifunctional because it is involved in both slow transport from the ERC and rapid internalization from the cell surface. IRAP's cytoplasmic domain also contains an additional, functionally redundant methionine-isoleucine–based internalization motif.

## MATERIALS AND METHODS

***TR Constructs.*** Overlapping oligonucleotide polymerase chain reaction was used to make all of the vpTR constructs using the HF polymerase kit (CLONTECH, Palo Alto, CA). To create these constructs, a plasmid encoding the cDNA clone of vpTR was used as a template (Johnson *et al.*, 1998). All constructs were created using overlapping primers encoding the mutations of interest. The final polymerase chain reaction product fragments were cut using *Eco*RV/*Hin*dIII and subcloned into the *Eco*RV/*Hin*dIII sites of pTM1010, thereby joining the chimeric construct with the remainder of the TR sequence (Johnson *et al.*, 1998). Oligonucleotides and restriction enzymes were purchased from Life Technologies-BRL (Rockville, MD). The transmembrane and cytoplasmic domains of the cDNA clones were sequenced using fluorescent ABI-sequencing techniques by the Rockefeller University DNA sequencing facility (New York, NY).

***Cell Lines.*** TRVb cells, a CHO cell line lacking functional endogenous hamster TR (McGraw *et al.*, 1987), were carried in McCoy's 5A medium containing 5% fetal bovine serum (FBS), penicillin-streptomycin, and 220 mM sodium bicarbonate, pH 7.2. The vpTR constructs were transfected into TRVb cells using Lipofectamine (Life Technologies-BRL). Cotransfection was performed with the plasmid pSV3-Neo as the dominant selectable marker. The ratio of chimeric DNA to pSV3-Neo was 10:1. Cells ($5 \times 10^5$ per 35-mm well) plated the previous day were incubated for 24 h in serum-free McCoy's medium containing the cDNA/Lipofectamine mixture. After 1 d in

McCoy's medium containing 5% FBS, the transfected cells were split into 100-mm stock plates containing McCoy's medium supplemented with 5% FBS and 1 mg/ml G418 (Gentecin, Life Technologies-BRL). G418-resistant clonal lines were isolated with cloning cylinders. Clonal lines were screened for expression of vpTR constructs by fluorescent transferrin uptake. The endocytic properties of the clonal lines were compared to cells expressing either the wild-type human TR (TRVb-1) or a mutant TR construct (TR Δ3-59) in which the cytoplasmic domain of the human TR is deleted (McGraw *et al.*, 1987; Johnson *et al.*, 1993).

***Ligands.*** Tf was purchased from Sigma (St. Louis, MO) and further purified by Sephacryl S-300 gel filtration. Iron-loaded diferric Tf and $^{125}$I-Tf were prepared as described previously (Yamashiro *et al.*, 1984). Horseradish peroxidase (HRP) was conjugated to iron-loaded transferrin as described previously (Mayor *et al.*, 1998).

***Trafficking Assays.*** The kinetic assays used to measure internalization and recycling rate constants and the steady-state distribution of the constructs between the interior and surface of cells have been described in detail elsewhere (Johnson *et al.*, 1993, 1998; Garippa *et al.*, 1994). These assays are briefly described below.

To measure the steady-state distribution between the surface and interior of cells, cells grown in a six-well cluster were incubated with 3 μg/ml $^{125}$I-Tf for 2 h at 37°C to achieve steady-state occupancy of the receptors. The cells were washed four times with 150 mM NaCl, 20 mM HEPES, 1 mM $CaCl_2$, 5 mM KCl, and 1 mM $MgCl_2$, pH 7.4 (med 1) at 4°C. The cells were incubated for 5 min at 4°C in 1 ml/well of 0.15 M NaCl and 0.02 M sodium citrate, pH 5.0, followed by 5 min at 4°C in med 1. This acid/neutral wash was repeated twice. These washes remove >90% of the Tf bound to the surface. The washes were pooled, and the radioactivity was measured. This value represents the Tf bound to the cell surface. The cells were solubilized, and the radioactivity was measured. This value represents the Tf in intracellular compartments. Two wells per plate were treated as the others except that a 200-fold excess of unlabeled Tf was added with the iodinated Tf. The radioactivity in the acid/neutral washes and associated with the cells represent nonspecific binding and was subtracted from the acid/neutral washes and from the cell-associated radioactivity, respectively.

To measure the internalization rate constant, cells grown in six-well clusters were incubated with 3 μg/ml $^{125}$I-Tf for 2, 4, 6, or 8 min. One cluster was used per time point. After the incubation time at 37°C the plates were placed on ice and washed four times with med 1 at 4°C. The cells were incubated for 5 min at 4°C in 1 ml/well of 0.15 M NaCl and 0.02 M sodium citrate, pH 5.0, followed by 5 min at 4°C in med 1. The cells were solubilized, and the radioactivity was measured. This value represents the Tf internalized during the incubation at 37°C. In parallel, a six-well cluster of cells was incubated in med 1 with 3 μg/ml $^{125}$I-Tf at 4°C for 2 h. The wells were washed four times with med 1, the cells were solubilized, and the radioactivity was determined. This value is the amount of TR or chimera on the surface. Two wells per plate were treated as the others except that a 200-fold excess of unlabeled Tf was added with the iodinated Tf. The average radioactivity in these wells is nonspecific binding and was subtracted from the average values of the other four wells per plate. The slope of a plot of the ratio of internal Tf to surface Tf (4°C binding) versus time is the internalization rate constant.

To measure the recycling rate constant, cells were incubated with 3 μg/ml iodinated Tf for 4 h at 37°C to achieve steady-state occupancy of the constructs with iodinated Tf. The cells were washed with med 1, incubated for 2 min at 37°C in 0.2 M NaCl and 50 mM MES, pH 5.0, followed by two washes with med 1. Incubation in the acidic medium releases Tf bound to TR on the cell surface. The cells were incubated at 37°C with 3 μg/ml unlabeled Tf and 100 μM iron chelator deferroxamine (efflux medium). At 1, 3, 5, 7, or 10 min the efflux medium was collected, and the cells were solubilized. The radioactivity in the efflux medium is the Tf released from the cells during the incubation, and the cell-associated radioactivity is the Tf remaining inside cells. Nonspecific binding was determined using a 200-fold excess of unlabeled Tf. The recycling rate constant is the slope of the natural logarithm of the percentage of Tf remaining associated with cells versus time.

***Colocalization of Cy3-Tf and NBD-SM.*** Cells grown on coverslip-bottom dishes were incubated with NBD-SM for 10 min at 37°C in serum-free medium, washed three times with serum-free medium, and chased for 30 min with 3 μg/ml Cy3-Tf at 37°C. After the chase, the cells were placed on ice and washed three times, 10 min each, with 5 mg/ml fatty acid-free BSA in med 1 to remove plasma membrane NBD-SM. The cells were fixed in 3.7% formaldehyde in med 1 before imaging.

Images were collected with an Axiovert 100M inverted microscope equipped with an LSM 510 laser scanning unit and a 63 × 1.4 NA plan Apochromat objective (Carl Zeiss, Thornwood, NY). To excite Cy3 and NBD fluorescence, 543 and 488 nm light were used, respectively. Emissions were selected with a 560-nm long pass filter for Cy3 or a 505- to 530-nm band pass filter for NBD. The NBD fluorescence was collected first; and then the NBD fluorescence was bleached before the Cy3 fluorescence was collected to prevent crossover.

***Fluorescence-quenching Assay.*** A fluorescence-quenching assay was used to measure the colocalization of fluorescein wheat germ agglutinin (F-WGA) with either the TR or vpTR. Cells grown on coverslip-bottom dishes were pulse-labeled with 50 μg/ml F-WGA (Sigma) for 5 min at 37°C in serum-free media and chased for 60 min with either an HRP-Tf conjugate or unlabeled transferrin. Cells were put on ice and washed with ice-cold med 1 and then incubated for 5 min with 0.1 M *N*-acetylglucasamine on ice to remove surface bound F-WGA, followed by two washes with med 1. To strip surface-bound Tf, cells were incubated for 5 min on ice in ice-cold citrate buffer (20 mM sodium citrate and 150 mM NaCl, pH 5.0), with one exchange of buffer, followed by two 5-min washes with ice-cold med 1. For the quenching reaction, cells were incubated with 25 μg/ml diaminobenzidine (DAB) and 0.0025% $H_2O_2$ in the dark for 30 min on ice, followed by two 5-min washes with ice-cold med 1. Finally, cells were fixed for 20 min with 3.7% formaldehyde in med 1.

Fluorescence microscopy was done with a DMIRB inverted microscope (Leica, Deerfield, IL), with a cooled charge-coupled device camera (Princeton Instruments, Trenton, NJ). Images were collected with either a 63 × 1.32 NA (for visualization) or a 40 × 1.25 NA (for quantification) oil immersion objective. Metamorph software (Universal Imaging, West Chester, PA) was used for image processing and quantification. The total fluorescein fluorescence per field was calculated by summing the pixel intensities over all cells in a field and subtracting a background fluorescence. To quantify the background fluorescence from nonspecific uptake of F-WGA, 0.1 M *N*-acetylglucasamine was added during the pulse-labeling with F-WGA.

To quantify the fluorescence in the endocytic recycling compartment of unquenched cells (no HRP) more specifically, a threshold intensity was chosen to separate the brightly labeled recycling compartment from the peripheral structures that were more dimly labeled with F-WGA. The mean fluorescence plus 1 SD, calculated for each field and averaged over all fields, was used as the threshold. The unquenched cells (no HRP-Tf) were used to calculate a threshold separately for each cell line. By visual inspection, the threshold separates the recycling compartment from peripheral structures. The fluorescence intensity was summed for all pixels with intensity above the threshold, and the same threshold was used for quenched and unquenched cells.

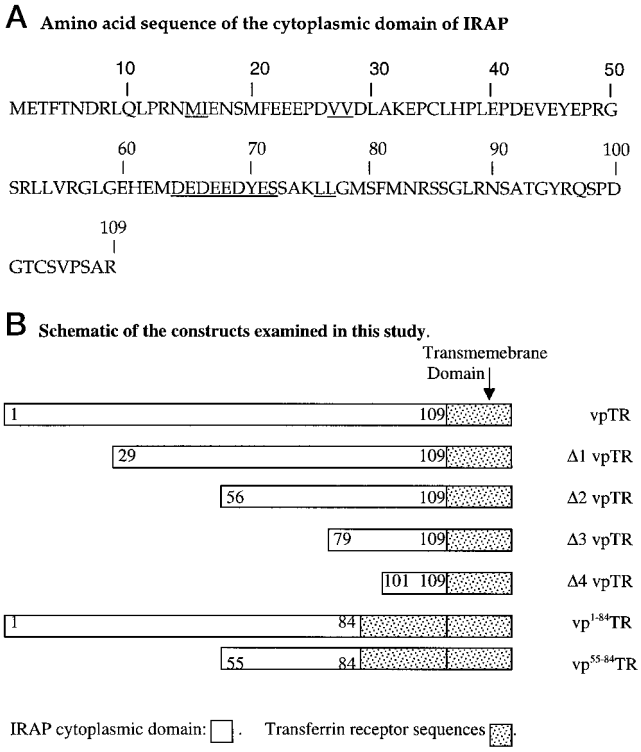


**Figure 1.** Cytoplasmic sequences of the vpTR constructs used in this study. (A) IRAP's cytoplasmic domain amino acid sequence is shown. Wild-type vpTR contains the entire 109-amino–terminal cytoplasmic domain of IRAP fused to the transmembrane and extracellular domains of the human TR (Johnson *et al.*, 1998). The numbers correspond to the position of residues from the amino terminus. The underlined residues have been mutated by alanine substitution and are discussed in the text. (B) Schematics of the deletion and substitution constructs are shown. The white-boxed regions are IRAP sequences and the numbers refer to the amino acid sequences of IRAP contained in the various constructs. The stippled regions are from the TR. All of the constructs contain the transmembrane and extracellular domains of the TR.

## RESULTS

### *Residues 1–54 Are Not Required for Dynamic Retention of IRAP*

We have previously shown that the 109-amino acid cytoplasmic domain of IRAP contains information required for IRAP's rapid internalization from the cell surface and its slow recycling back to the plasma membrane from the general ERC (Johnson *et al.*, 1998). As a first step toward identifying the trafficking motifs within IRAP's cytoplasmic domain, we characterized the behaviors of a set of four incremental amino-terminal truncations of the IRAP sequences in the vpTR chimera (Figure 1). These constructs were transfected into TRVb CHO cells, a cell line that does not express functional endogenous hamster TR (McGraw *et al.*, 1987). A number of clonal lines for each construct were examined. There were no significant differences among clonal lines expressing the same construct. The endocytic behaviors of the deletion constructs were compared with that of vpTR (Johnson *et al.*, 1998), the wild-type human TR

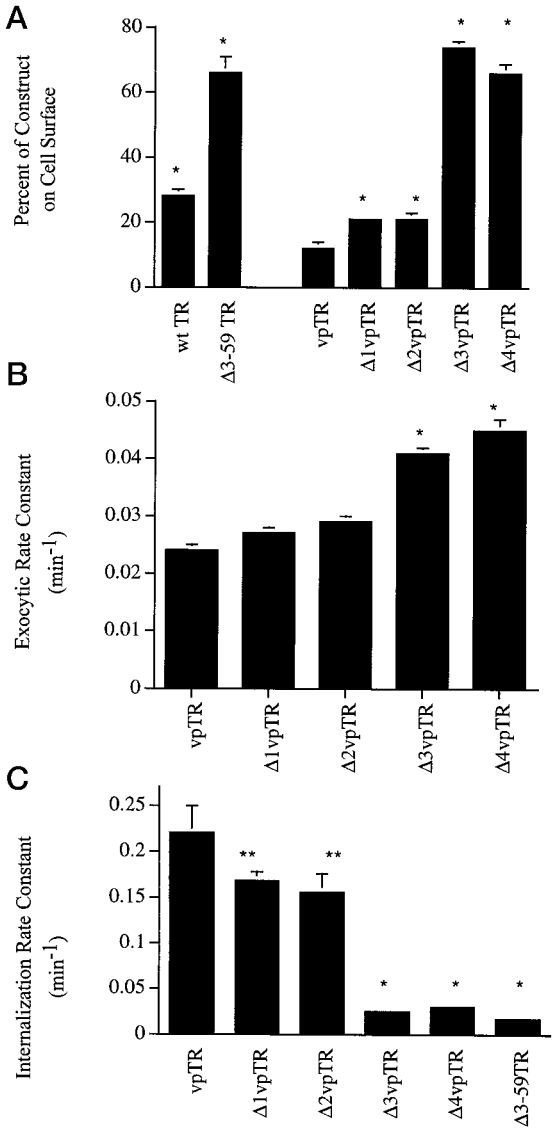


**Figure 2.** Endocytic trafficking kinetics of the amino-terminal deletion vpTR constructs. (A) Percentage of vpTR deletion constructs on the cell surface at steady state. The results shown are the average values ± SEM from at least three independent determinations. (B) The average recycling rate constants from at least four independent determinations ± SEM are presented. (C) The average internalization rate constants from at least four independent determinations ± SEM are shown. The data are from representative clonal lines expressing the various constructs. The values noted by an asterisk are different from the corresponding value for vpTR with $P$ values $<$ 0.001 (heteroscedastic, two-tailed Student's $t$ test). The internalization rate constants of Δ1 and Δ2vpTR differ from the internalization rate constant of vpTR with a $P < 0.1$, noted by a double asterisk (heteroscedastic, two-tailed Student's $t$ test).

(McGraw *et al.*, 1987), and a cytoplasmic deletion mutant of the human TR (Δ3-59TR) (Johnson *et al.*, 1993).

The percentage of the deletion constructs on the cell surface at steady state were determined (Figure 2A). As we have previously shown, ~35% of TR, 70% of Δ3-59 TR, and

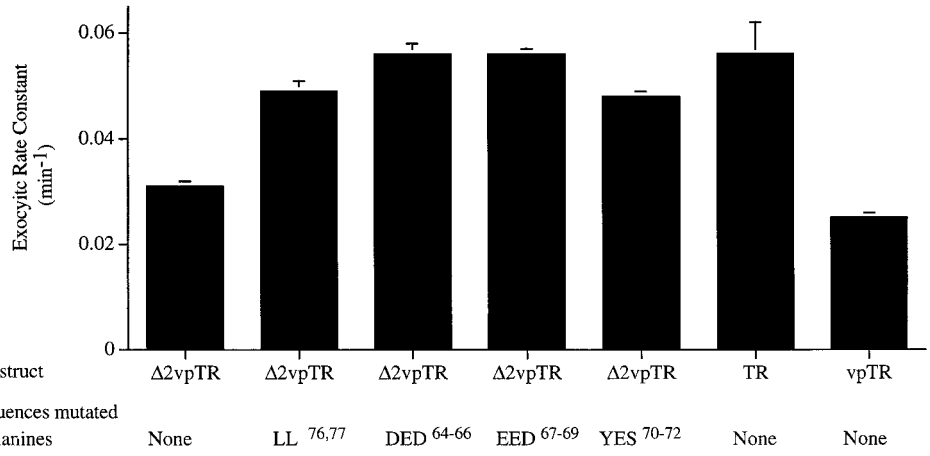


**Figure 3.** Recycling kinetics of Δ2 vpTR constructs containing point mutations in LL[76–77] or the cluster of acidic amino acids. The average recycling rate constants ± SEM from at least three independent determinations are presented. The data are from representative clonal lines expressing the various constructs. The recycling rate constants of TR and vpTR are presented for comparison. The recycling rate constants of the mutants in the Δ2vpTR background are all different from the recycling rate constant of ΔvpTR with $P$ values $< 0.001$ (heteroscedastic, two-tailed Student's $t$ test).

<15% of vpTR are on the cell surface, reflecting differences in the rates of internalization and recycling among these proteins. A smaller fraction of vpTR is on the surface because it is internalized at the rapid rate of the TR, but recycled at one-third the rate of the TR (Johnson *et al.*, 1998). A greater percentage of Δ3-59 TR is on the cell surface because it is internalized at one-tenth the rate but returned to the surface at the same rate as the TR (Jing *et al.*, 1990; Johnson *et al.*, 1993). The steady-state distributions of Δ3 and Δ4 vpTR are similar to the distribution of the Δ3-59 TR, a protein that traffics like a bulk membrane marker (Mayor *et al.*, 1993). These data indicate that the region between amino acids 56 and 78 (the region between Δ2 vpTR and Δ3 vpTR) is most important for determining the distribution of vpTR. The distributions of both Δ1 and Δ2 vpTR are also shifted toward the cell surface. Although these changes are less than that observed for the other deletions, these small differences are statistically significant (Student's $t$ test, $P < 0.0001$). The altered distribution of Δ1 vpTR demonstrates that sequences within the first 28 amino acids of IRAP influence trafficking to a minor extent. To determine which endocytic parameters are affected by the deletions, the internalization and recycling rate constants were measured (Figure 2B). Both Δ3 and Δ4 vpTR are recycled back to the cell surface more rapidly than vpTR. The recycling rate constants for Δ3 and Δ4 vpTR are similar to the recycling rate constant of the TR. The Δ1 and Δ2 vpTR constructs are recycled slowly, at rates similar to the recycling rate of vpTR. The Δ3 and Δ4 vpTR are recycled at rates similar to the TR, indicating that the region between amino acids 56 and 78 contains information that is required for the slow recycling of vpTR. These data confirm our previous finding that LL[76,77] is necessary for slow recycling of vpTR, because this sequence is deleted in the Δ3 vpTR construct (Johnson *et al.*, 1998). Both Δ3 and Δ4 vpTR are internalized at the same slow rate of TR Δ3-59, demonstrating that Δ3 and Δ4 vpTR are internalized by a nonconcentrative mechanism (Figure 2C). These data indicate that the sequences between amino acids 56 and 78 play an important role in rapid internalization of vpTR. The rapid recycling and slow internalization of the Δ3 and Δ4 vpTR account for the shift in steady-state distribution of these constructs toward the surface (Figure 2A). Although the Δ1 and Δ2 vpTR constructs are internalized considerably more rapidly than the Δ3 and Δ4 vpTR constructs, they are internalized ~20% slower than the wild-type vpTR. Supporting the validity of these small changes in internalization are the data that the steady-state distribution of Δ1 and Δ2vpTR are shifted toward the surface. Although individually the significance of these small changes in Δ1 and Δ2vpTR may be questioned, taken together these data indicate that the sequences between residues 1 and 29 (i.e., deleted in Δ1 vpTR) have an effect on the rate of IRAP's internalization.

### *A Cluster of Acidic Residues Adjacent to LL[76,77] Are Important for Slow Recycling and Rapid Internalization of vpTR.*

The data in Figure 2 demonstrate that Δ2 vpTR contains the primary information necessary for the characteristic trafficking of vpTR. To further define the sequences required for rapid internalization and slow recycling, we analyzed the behaviors of a series of point mutations in the Δ2 vpTR background. The region between amino acids 56 and 78 contains several potential endocytic trafficking motifs, including the previously characterized LL[76,77] (Johnson *et al.*, 1998) and a cluster of acidic amino acids (Figure 1). There is a tyrosine residue at position 70, although the surrounding sequences do not conform to the typical aromatic based motif (Collawn *et al.*, 1990). To examine the role of these sequences in trafficking of IRAP, the following mutations in the Δ2 vpTR construct were made and their endocytic behaviors characterized: substitution of three alanines for DED[64–66], or EED[67–69] or YES[70–72], and substitution of two alanines for LL[76,77] (Figure 1).

All three of the mutations in the cluster of acidic residues as well as the LL[76,77]AA mutation in the Δ2 vpTR background are recycled at the same rapid rate as the TR, which is approximately twice the rate of the Δ2 vpTR construct (Figure 3). Thus, both the acidic cluster, DEDEEDYES[64–72] and the LL[76,77] are required elements of the motif that slows recycling back to the cell surface. The finding that slow recycling of Δ2 vpTR requires LL[76,77] indicates that the same motif that regulates full-length vpTR trafficking also regulates Δ2 vpTR trafficking (Johnson *et al.*, 1998).

The internalization rate constants of the various Δ2 vpTR mutants were also measured. The Δ2 vpTR-LL[76,77]AA con-

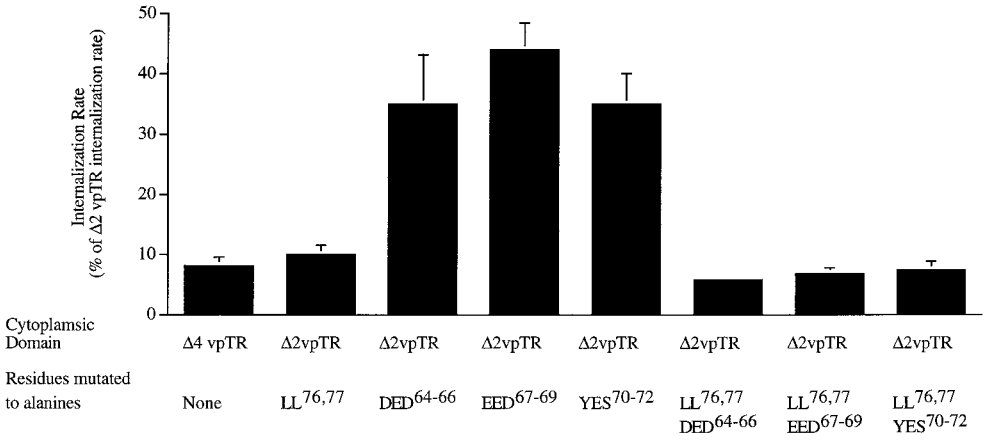


**Figure 4.** Internalization kinetics of Δ2 vpTR constructs containing point mutations in $LL^{76-77}$ or the cluster of acidic amino acids. The internalization rates of the mutant constructs are expressed as percentages of the internalization rate of Δ2 vpTR. The data are the averages ± SEM from at least three independent determinations. The internalization rate of Δ4 vpTR, expressed as a percentage of Δ2 vpTR, is presented as a measure of the nonconcentrative internalization rate. The internalization rates constants for Δ2vpTR-$DED^{64-66}$, Δ2vpTR-$EED^{67-69}$, and Δ2vpTR-$YES^{70-72}$ are different from the internalization rate constant of Δ2vpTR and from the rate for Δ4 vpTR with $P$ values $< 0.001$ (heteroscedastic, two-tailed Student's $t$ test).

struct is internalized at the same slow rate as the Δ4 vpTR construct, which is the rate characteristic of nonconcentrative internalization (Figure 4). This is a surprising result because we have previously shown that the $LL^{76,77}AA$ mutation in the context of the complete cytoplasmic domain of IRAP does not affect internalization (Johnson *et al.*, 1998). These data indicate that information in the region 1 to 54 of IRAP's cytoplasmic domain (i.e., the region deleted in the Δ2 construct) can compensate for the loss of $LL^{76,77}$ in promoting rapid internalization. Mutation of $DED^{64-66}$, $EED^{67-69}$, or $YES^{70-72}$ slows internalization of Δ2 vpTR by ~50% (Figure 4). The quantitative difference in the internalization of the $LL^{76,77}$ and acidic cluster mutants indicates that $LL^{76,77}$ is more important for rapid internalization of Δ2 vpTR. Constructs with combined mutations in the $LL^{76,77}$ and the acidic sequences are internalized at the slow rate characteristic of nonconcentrative internalization (Figure 4). Thus, both the $LL^{76,77}$ and the acidic cluster are elements of the IRAP internalization motif located between residues 56 and 78. This analysis does not distinguish the possibility that the cluster of acidic amino acids and the di-leucine are elements of a single internalization motif from the possibility that $LL^{76,77}$ and the acidic cluster are elements of distinct internalization motifs (see below).

### *Mutation of the Cluster of Acidic Residues Increases Recycling but Does Not Affect Internalization of Full-Length vpTR*

We next examined the effects of mutating the cluster of acidic amino acids in the context of the complete cytoplasmic domain of IRAP. Mutation of $DED^{64-66}$, $EED^{67-69}$, or $YES^{70-72}$ increases the recycling of vpTR to the rapid rate observed for vpTR-$LL^{76,77}AA$ and the TR (Figure 5A). These results demonstrate that the cluster of acidic residues, $DEDEEDYES^{64-72}$, and the $LL^{76,77}$ are essential elements of the motif that slows recycling. Thus, mutations that affect recycling of the Δ2 vpTR have the same effect on trafficking when examined in the context of the complete cytoplasmic domain of IRAP. This is not the case when the effects of these mutations on internalization are examined in the context of

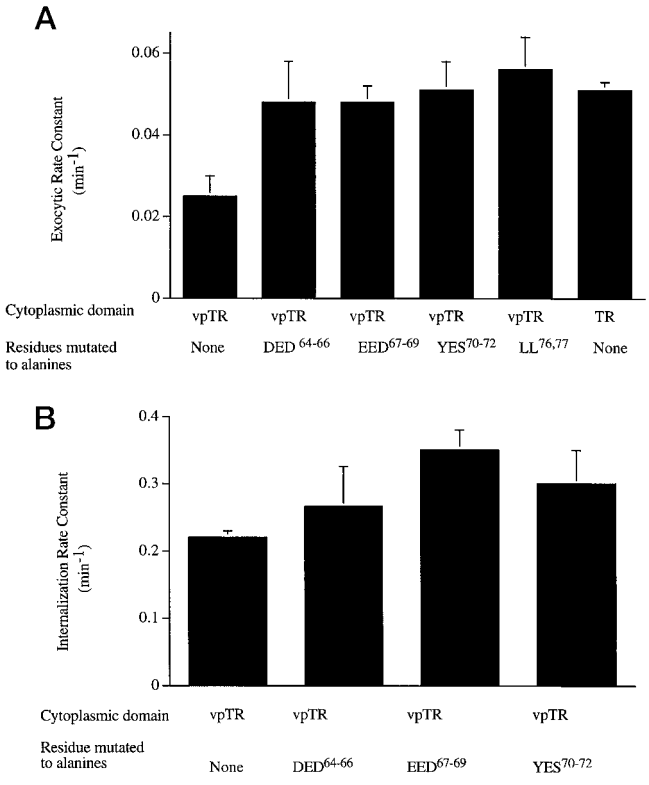


**Figure 5.** Endocytic trafficking kinetics of the mutations in the cluster of acidic residues in the full-length IRAP cytoplasmic domain. (A) The average recycling rate constants of vpTR constructs containing point mutations in the acidic sequences. The average recycling rate constants from at least three independent determinations ± SEM are presented. The internalization rate constants of vpTR and vpTR $LL^{76,77}AA$ are presented for comparison. The exocytic rate constants for the various mutants of vpTR are all different from the exocytic rate constant of vpTR with a $P < 0.001$ (heteroscedastic, two-tailed Student's $t$ test). (B) The average internalization rate constants from at least three independent determinations ± SEM are presented. Data are from representative clonal cell lines expressing the indicated constructs.

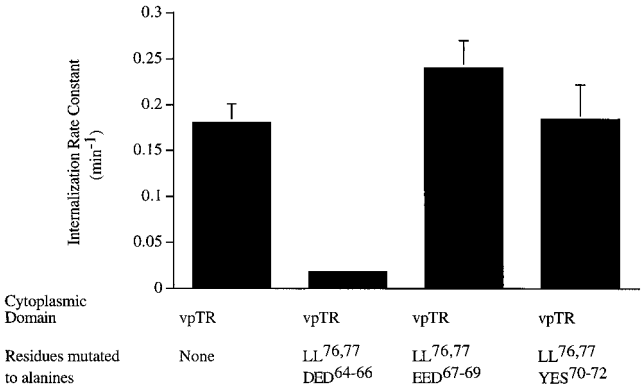


**Figure 6.** Internalization rate constant measurements of full-length vpTR containing mutations in both the cluster of acidic resides and $LL^{76-77}$. The average internalization rate constants from at least three independent determinations ± SEM are presented. Experiments were performed on representative clonal cell lines expressing the indicated constructs. The internalization rate constant of vpTR is presented for comparison.

the complete cytoplasmic domain of IRAP. The vpTR constructs with mutations in the cluster of acidic residues are rapidly internalized (Figure 5B), whereas these same mutations in Δ2 vpTR slow internalization (Figure 4). As noted previously, the same is true for mutation of $LL^{76,77}$, which is required for rapid internalization of Δ2 vpTR but dispensable in the vpTR background. These data indicate that there is an internalization motif located between residues 1 and 55 (i.e., the region deleted in Δ2 vpTR) that can promote rapid internalization when either the $LL^{76,77}$ or the DEDEEDYES acidic cluster is mutated.

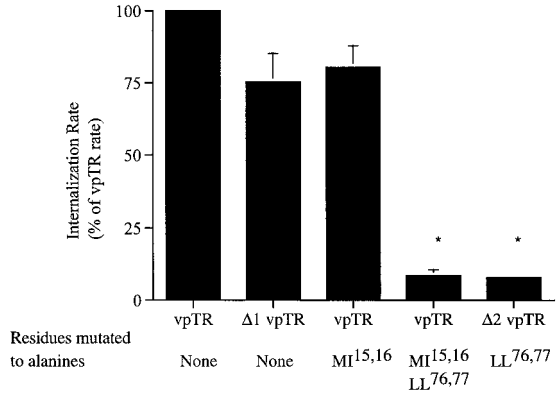


**Figure 7.** Internalization rate constant measurements of full-length vpTR containing mutations in $MI^{15,16}$ or in both $MI^{15,16}$ and $LL^{76-77}$. The data are presented as percentages of the internalization rate of vpTR. The data for Δ1 vpTR and Δ2 vpTR$LL^{76,77}$AA are presented for comparison. Experiments were performed on representative clonal cell lines expressing the indicated constructs. The internalization rate constant of vpTR $MI^{15,16}$ differs from that of vpTR with a $P < 0.1$ (heteroscedastic, two-tailed Student's $t$ test). The values noted by the asterisk differ from the internalization rate constant of vpTR with $P < 0.001$.

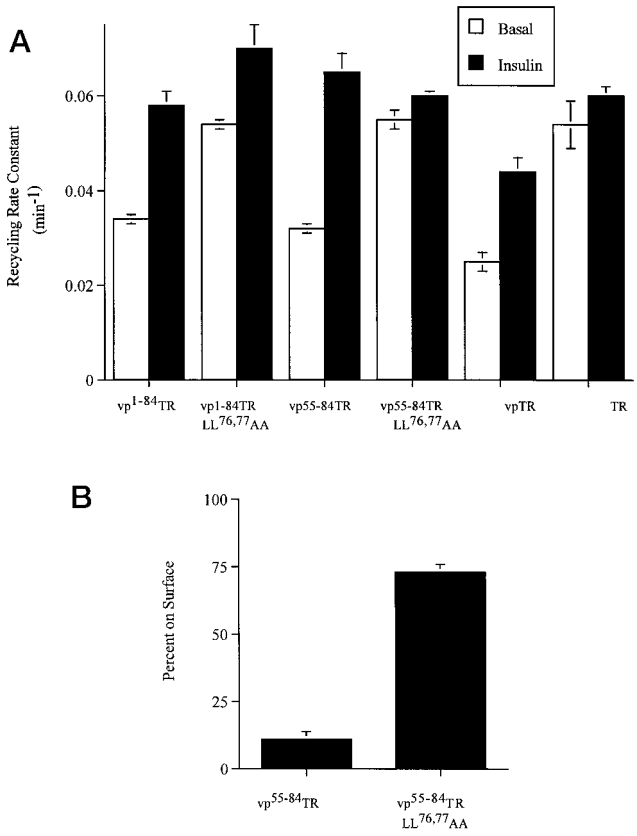


**Figure 8.** Endocytic trafficking kinetics of $vp^{1-84}$TR and $vp^{55-84}$TR constructs. (A) The average ± SEM recycling rate constants determined in at least three independent measurements are shown. The internalization rate constants of vpTR and TR are shown for comparison. ■, measured in the absence of insulin; □, from cells incubated with 500 nM insulin. (B) Percentage of vpTR deletion constructs on the cell surface. The results shown are the average values ± SEM from at least three independent determinations.

To further investigate the sequences required for internalization, we examined constructs in which both the acidic cluster and $LL^{76,77}$ were mutated in the context of the complete cytoplasmic domain of IRAP. Constructs containing mutations of $EED^{67-69}$ or $YES^{70-72}$ along with the $LL^{76,77}$AA mutation are rapidly internalized, whereas mutation of both $DED^{64-66}$ and $LL^{76,77}$ reduces internalization by 10-fold (Figure 6). These data demonstrate that the region between residues 56 and 78 contains two independent internalization motifs, one based on $DED^{64-66}$ and the other based on the $LL^{76,77}$. When both of these motifs are mutated, the internalization rate of vpTR is reduced to levels observed for proteins internalized by nonconcentrative mechanisms.

We have previously shown that the $LL^{53,54}$AA mutation has no effect on internalization or recycling (Johnson *et al.*, 1998). As a control for the specific role of the $LL^{76,77}$ in internalization we examined the behaviors of constructs with the $DED^{64-66}$, $EED^{67-69}$, or $YES^{70-72}$ mutations in the $LL^{53,54}$ AA background. These constructs are all rapidly internalized, confirming a specific role for $LL^{76,77}$ (Johnson, Lampson, and McGraw, unpublished results).

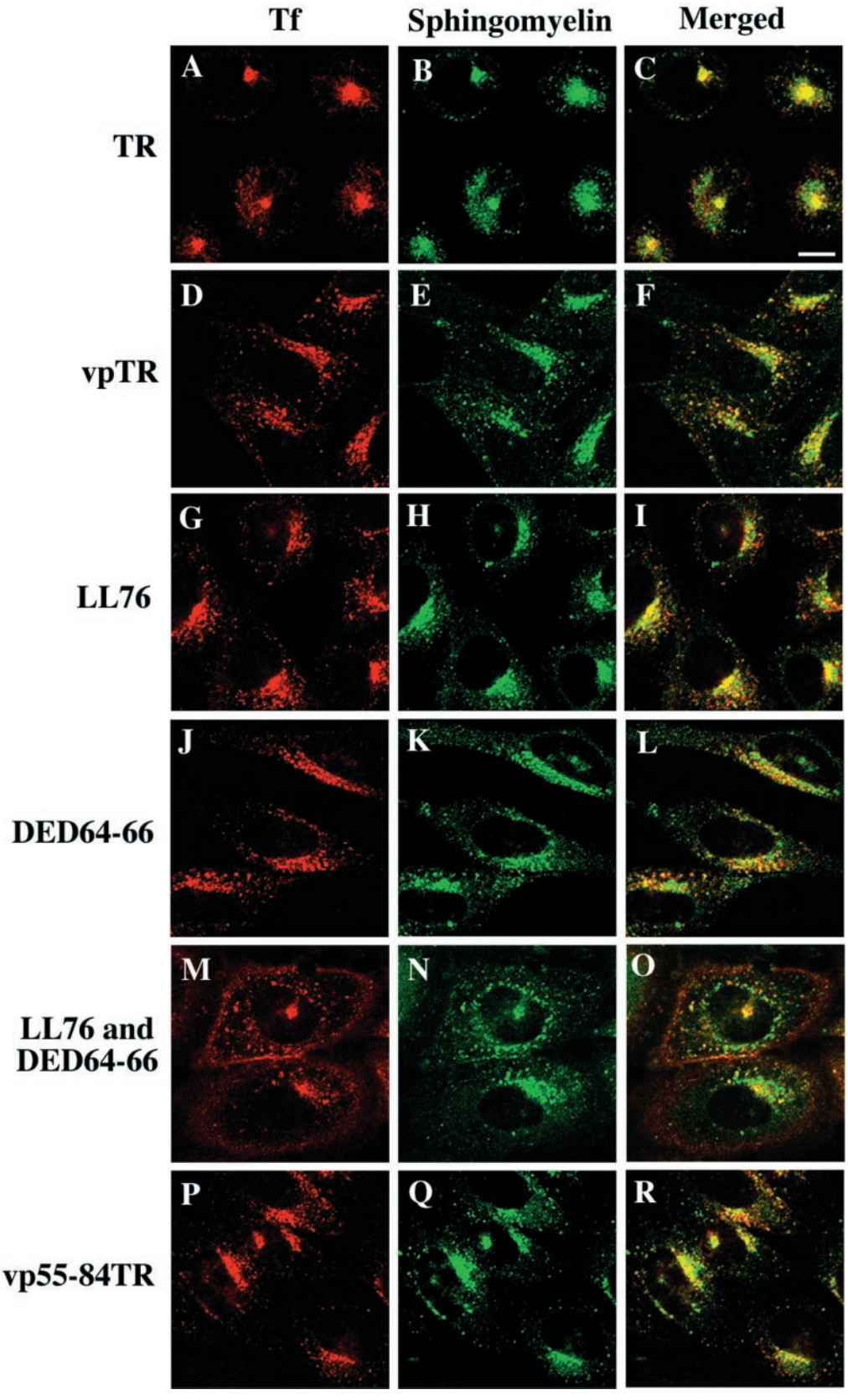
Tf
Sphingomyelin
Merged
TR
vpTR
LL76
DED64-66
LL76 and DED64-66
vp55-84TR
A
B
C
D
E
F
G
H
I
J
K
L
M
N
O
P
Q
R

### *A Met-Ile Sequence Is a Third Internalization Motif in the Cytoplasmic Domain of IRAP*

Deletion of the first 28 amino acids in the cytoplasmic domain of IRAP reduces internalization of vpTR (Figure 2). There are two potential di-nonpolar internalization motifs in this region: $MI^{15,16}$ and $VV^{27,28}$. Mutation of $VV^{27,28}$ to AA does not affect internalization, whereas mutation of $MI^{15,16}$ to AA reduces internalization to the intermediate rate observed for Δ1 vpTR (Figure 7). These results are consistent with the slow internalization of Δ1 and Δ2 vpTR mutants being due to the loss of the $MI^{15,16}$-based internalization motif. Both vpTR $MI^{15,16}$AA and vpTR $VV^{27,28}$AA are recycled at the same slow rate as vpTR, demonstrating that neither of these sequences contributes to the slow recycling of IRAP.

Because the effect of the $MI^{15,16}$AA mutation on internalization is small, it was of interest to determine the behavior of a construct in which the $MI^{15,16}$ sequence and one of the other sequences important for internalization are both mutated. For example, analyses of the Δ2 vpTR constructs indicated that $DED^{64-66}$ and $LL^{76,77}$ are important for rapid internalization and that sequences within the first 28 amino acids influence the functioning of these motifs in maintaining rapid internalization (Figure 6). The behavior of vpTR $MI^{15,16}$AA indicates that the $MI^{15,16}$ sequences influence internalization. An interpretation of these data is that rapid internalization of IRAP is determined by three distinct motifs: $DED^{64-66}$, $LL^{76,77}$, or $MI^{15,16}$. These findings indicate that two of the three motifs are required for rapid internalization of vpTR. To test his hypothesis we examined the internalization rate of a mutant in which both $MI^{15,16}$ and $LL^{76,77}$ were mutated to AA. This double mutant construct is internalized at one-tenth the rate of vpTR, consistent with the proposal that two of the three internalization sequences are necessary for rapid internalization of vpTR (Figure 7). The large change in internalization of vpTR mutated in $MI^{15,16}$ and $LL^{76,77}$ sequences provides more compelling evidence for a role of $MI^{15,16}$ in internalization of IRAP than the behavior of the $MI^{15,16}$AA mutant alone.

### *Residues 55 to 84 Are Necessary and Sufficient for Dynamic Retention of IRAP*

In analysis of the deletion mutants discussed above we have shown that the sequences of IRAP's cytoplasmic domain between 1 and 54 are not required for the slow recycling characteristic of IRAP trafficking. To delineate the carboxyl boundary of the sequences that regulate recycling of IRAP, we made a construct, $vp^{1-84}$TR, in which we substituted the membrane proximal 25 amino acids of the TR for the juxtamembrane 25 amino acids of IRAP (Figure 1B). Because residues between 1 and 54 are not essential for the specialized trafficking of IRAP, we also made a construct, $vp^{55-84}$TR, in which the first 54 amino acids of $vp^{1-84}$TR were deleted. In these constructs the $LL^{76,77}$/acidic cluster are the same number of amino acids from the membrane as in IRAP. The recycling rate constants of both these constructs are similar to the slow recycling rate constant characteristic of vpTR (Figure 8A), demonstrating that IRAP residues between 84 and 109 do not contribute to the slow recycling characteristic of IRAP trafficking. Mutation of $LL^{76,77}$ to AA in both of these constructs increases their recycling rate constants to the rapid rate characteristic of the TR (Figure 8A). These findings are consistent with the behavior of the $LL^{76,77}$AA mutation in the complete cytoplasmic domain of IRAP and thereby establish that the same information that regulates the recycling rate of vpTR also regulates the recycling rate of the $vp^{55-84}$TR and $vp^{1-84}$TR constructs.

The behavior of the $vp^{55-84}$TR construct indicates that the residues between 55 and 84 are necessary and sufficient for dynamic retention of IRAP. To establish that this is the case, we measured the surface-to-internal distribution and the internalization rate constant for $vp^{55-84}$TR and the $vp^{55-84}$TR -$LL^{76,77}$AA mutant. The $vp^{55-84}$TR construct has the same distribution as vpTR (Figure 8B) and is internalized at the same rapid rate as vpTR, whereas the $LL^{76,77}$AA mutant is slowly internalized and has a distribution characteristic of a protein trafficked by a bulk membrane endocytosis. Thus, all the information that is required for trafficking characteristic of IRAP is contained within resides 55 to 84 of IRAP's cytoplasmic domain. The slow internalization of the $LL^{76,77}$ AA mutant is consistent with our analysis of IRAP's internalization motifs because the $LL^{76,77}$-based motif is required for rapid internalization in the absence of $MI^{15,16}$.

An additional characteristic of the dynamic retention of vpTR is that its recycling rate constant is increased approximately twofold by insulin (Johnson *et al.*, 1998). The effect of insulin on the recycling of vpTR is not a result of changes in the kinetics of general recycling, because insulin does not affect the recycling rate constant of the TR (Johnson *et al.*, 1998). Insulin increases the recycling rate constant of $vp^{55-84}$TR by approximately twofold, whereas insulin has no effect on the recycling rate constant of the $LL^{76,77}$AA mutant construct (Figure 8B). These data demonstrate that the 29 amino acids between 55 and 84 contain all the information required for specialized trafficking of IRAP. In addition, these data are consistent with our previous finding that insulin only effects the recycling of vpTR constructs that are slowly recycled in the absence of insulin.

### *IRAP Is Dynamically Retained in the Endocytic Recycling Compartment*

Development of a model for the dynamic retention of IRAP depends on the intracellular compartment in which the protein is retained. IRAP could be retained either in the general ERC, as we have previously proposed (Johnson *et al.*, 1998), or by sorting to a distinct, "slow" recycling compartment. To distinguish between these models, we used two different methods to measure colocalization with markers for the ERC: a morphological analysis and a more rigorous, quantitative fluorescence-quenching assay. If both the TR and vpTR colocalize to the same extent with markers for the

**Figure 9 (facing page).** Colocalization of NBD-SM and Cy3-Tf. Uptake of NBD-SM (green) and Cy3-Tf (red) is shown in cells expressing the TR (A–C), vpTR (D–F), $LL^{76,77}$AA mutant (G–I), $DED^{64-66}$AAA mutant (J–L), $LL^{76,77}$AA and $DED^{64-66}$AAA double mutant (M–O), or $vp^{55-84}$TR (P–R) constructs. Scale bar, 10 μm. Images are single optical sections (1-μm thickness) from the confocal microscope.

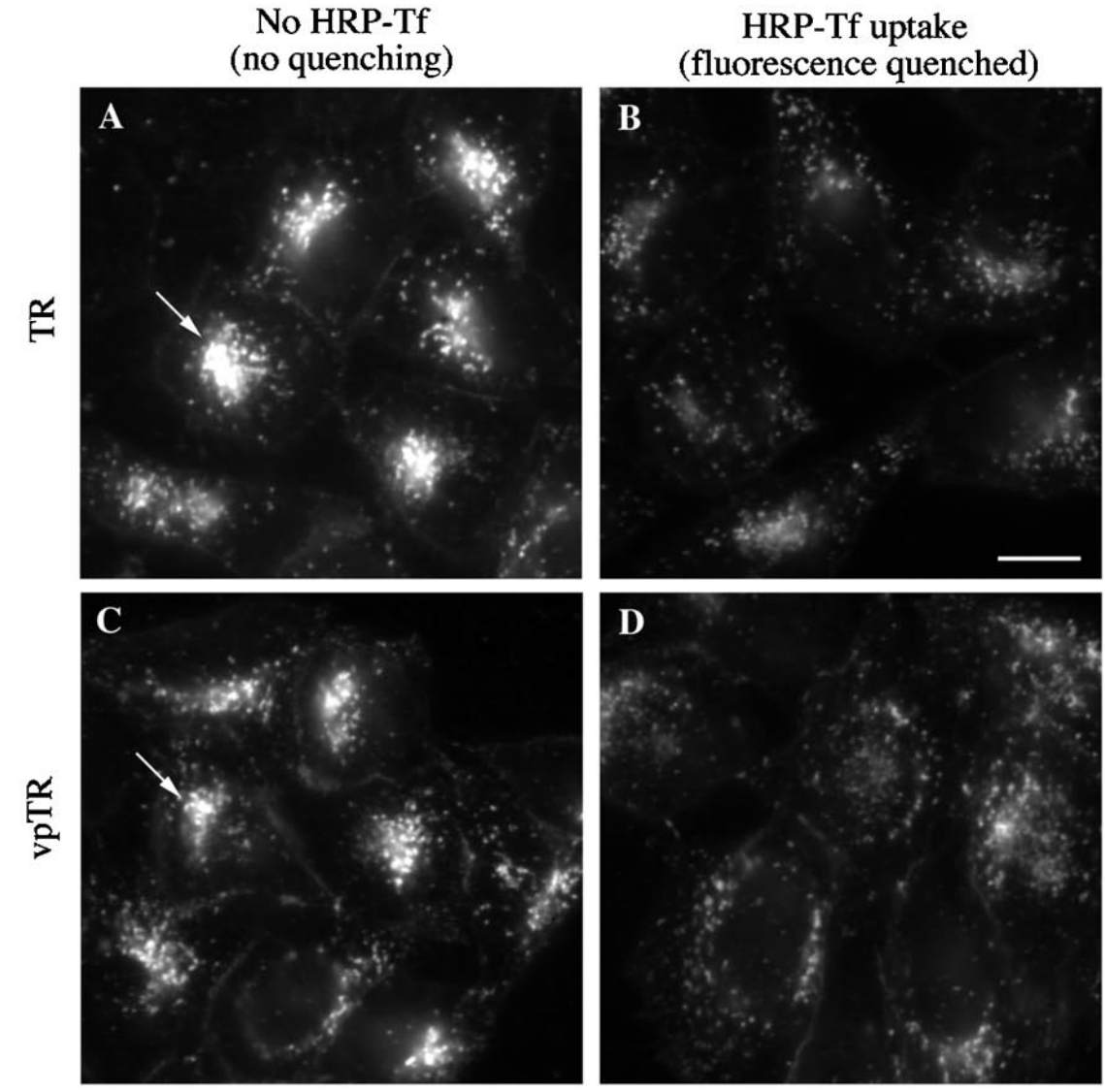
No HRP-Tf
(no quenching)
HRP-Tf uptake
(fluorescence quenched)
A
B
C
D
TR
vpTR

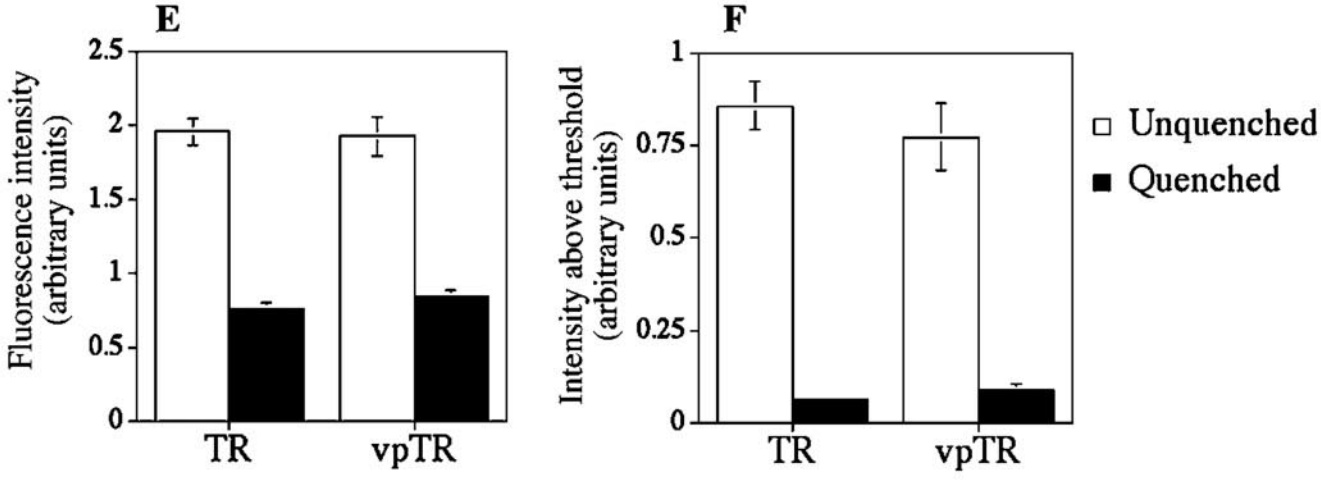
E
Fluorescence intensity
(arbitrary units)
2.5
2
1.5
1
0.5
0
TR
vpTR
F
Intensity above threshold
(arbitrary units)
1
0.75
0.5
0.25
0
TR
vpTR
Unquenched
Quenched

ERC, then we can conclude that the ERC is the retention compartment.

First we used fluorescent sphingomyelin as a marker for the ERC. Colocalization of internalized molecules with sphingomyelin internalized from the plasma membrane has been used to establish localization in the ERC of CHO cells (Koval and Pagano, 1989, 1990; Mayor *et al.*, 1993; Presley *et al.*, 1997). We have previously shown that both the TR and vpTR colocalize with sphingomyelin (Johnson *et al.*, 1998). As shown in Figure 9, we tested a number of vpTR mutations, which have varying effects on trafficking, and all of these colocalize with sphingomyelin. These constructs include the $LL^{76,77}AA$ and $DED^{64-66}AAA$ mutants, which are rapidly recycled, the $LL^{76,77}AA$ and $DED^{64-66}AAA$ double mutant, which is slowly internalized, and $vp^{55-84}TR$, which includes the necessary and sufficient residues for dynamic retention. The intracellular distributions of these constructs are similar to the TR and vpTR; all have the characteristic pericentriolar distribution of the ERC in CHO cells. The $LL^{76,77}AA$ and $DED^{64-66}AAA$ double mutant is also clearly visible on the cell surface, as expected for a protein that is slowly internalized. These data demonstrate that mutations that change the trafficking characteristics of vpTR do not change its intracellular localization. Both slowly and rapidly recycled constructs colocalize with sphingomyelin in the ERC.

As a more rigorous test of the colocalization of the TR and vpTR, we used a quantitative fluorescence-quenching assay, which has been used previously to show colocalization of proteins in the endosomal system (Ghosh *et al.*, 1998; Mayor *et al.*, 1998). The quenching reaction is catalyzed by HRP, which is conjugated to Tf and internalized by either the TR or vpTR. With the addition of DAB and $H_2O_2$, a dense reaction product is formed, which does not extend beyond the compartment containing the HRP. Fluorophores in the compartment are quenched by the reaction product, whereas those in separate compartments are unaffected. The assay can therefore distinguish between compartments that are separate but spatially too close for resolution by light microscopy.

We used fluorescien wheat germ agglutin (F-WGA) as a marker for the ERC (Raub *et al.*, 1990) and either the TR or vpTR to deliver HRP-Tf. F-WGA colocalizes as expected with Cy3-Tf taken up by either the TR or the vpTR. As shown in Figure 10, F-WGA intensely labels the ERC, with less intense labeling of punctate peripheral structures, as reported previously (Raub *et al.*, 1990). Quenching of the F-WGA fluorescence is also shown in Figure 10 in cells that have taken up HRP-Tf or in control cells (no HRP). The fluorescence in the pericentriolar compartment (arrows) is clearly quenched, whereas more peripheral structures, which are not part of the ERC, are relatively unaffected.

We quantified the extent of quenching by summing the total fluorescence intensity per field. This analysis shows that HRP-Tf delivered by either the TR or vpTR quenches the F-WGA fluorescence equally, indicating that vpTR and TR are equally distributed among the WGA-containing endosomal compartments. These data support our proposal that vpTR is retained in the ERC (Figure 10E). The quenching is not complete because the peripheral WGA-containing structures, which contain neither vpTR nor TR, are not quenched. To quantify the fluorescence in the ERC more specifically, we used a threshold intensity to distinguish between the bright ERC and dimmer peripheral structures (see MATERIALS AND METHODS). By summing the intensity above this threshold, we get a more accurate estimate of fluorescence concentrated in the ERC. By this analysis, almost all of the F-WGA fluorescence in the ERC is quenched by either the TR or vpTR (Figure 10F). These data demonstrate that the TR and vpTR are contained in the same intracellular compartment as F-WGA and, therefore, in the same compartment as each other. Because we know that the TR is in the ERC, we can conclude that vpTR is dynamically retained in the ERC rather than by sorting to a distinct compartment.

## DISCUSSION

We have used a chimera between IRAP and the TR as a reporter molecule in studies of the molecular mechanism of dynamic retention in the ERC of CHO fibroblast cells. Dynamic retention of IRAP is achieved by rapid internalization from the plasma membrane and slow transport from the ERC back to the cell surface (Johnson *et al.*, 1998). Here we show that a 29-amino acid region of IRAP's cytoplasmic domain, residues 55 to 84, is necessary and sufficient for dynamic retention. A cluster of acidic amino acids ($DEDEEDYES^{64-72}$) and a di-leucine sequence ($LL^{76,77}$) within this region are required elements of the motif that slows recycling of IRAP from the ERC back to the cell surface. The acidic cluster/di-leucine–based motif functions in the complete cytoplasmic domain of IRAP, when residues 1 to 55 of IRAP are deleted, and when residues 55 to 84 of IRAP are transferred to the TR. These data indicate that the information that is required for the slow recycling of IRAP is restricted to the 29-amino acid region from 55 to 84.

Interpretation of the data for rapid internalization of IRAP is more complicated. Three sequences play a role in rapid internalization: $DED^{64-66}$, $LL^{76,77}$, and $MI^{15,16}$. The $LL^{76,77}$ and $DED^{64-66}$ sequences are also elements of the motif that slows recycling. Any one of the three sequences can be mutated in the complete cytoplasmic domain of IRAP without reducing internalization of vpTR to the rate observed for bulk membrane uptake, whereas mutation of two of these motifs reduces internalization by 10-fold. These data indicate that any two of the three internalization motifs are required for rapid internalization and we have shown this to

**Figure 10 (facing page).** Colocalization of the TR or vpTR with F-WGA shown by fluorescence quenching. Cells were labeled with F-WGA, incubated with either HRP-Tf or unlabeled Tf, and processed for DAB cytochemistry to quench the F-WGA fluorescence as described in MATERIALS AND METHODS. (A–D) F-WGA fluorescence with no HRP and no quenching (A and C) or after quenching due to HRP-Tf uptake (B and D) in cells expressing the TR (A and B) or vpTR (C and D). Arrows, recycling compartments labeled with F-WGA. Scale bar, 10 $\mu$m. (E) Total fluorescence intensity per field in cells with or without HRP-Tf uptake (mean $\pm$ SE, $N = 10$ fields, >20 cells per field). (F) Fluorescence intensity per field above a threshold in cells with or without HRP-Tf uptake. The threshold was chosen to include the recycling compartments but exclude peripheral fluorescence (explained in MATERIALS AND METHODS).

be the case by examining the behaviors of constructs mutated in both $MI^{15,16}$ and $LL^{76,77}$ or $DED^{64-66}$ and $LL^{76,77}$. We have not directly examined the effect of mutating both $MI^{15,16}$ and $DED^{64-66}$. The significance of the redundancy in internalization motifs is not clear at this time; however, this is not unique to IRAP, because a number of membrane proteins are known to have multiple, functionally redundant internalization motifs.

A complication in interpreting the data on internalization of the various mutants is that in the Δ2 vpTR background mutation of $DED^{64-66}$, $EED^{67-69}$, or $YES^{70-72}$ reduce internalization, whereas in the complete cytoplasmic domain only the $DED^{64-66}$ $LL^{76,77}$ double mutant is slowly internalized. Both the $EED^{67-69}$ $LL^{76,77}$ and the $YES^{70-72}$ $LL^{76,77}$ double mutants are rapidly internalized. In the absence of structural information it is difficult to reconcile all of these observations, although an interpretation of the data is that, in the Δ2 vpTR truncation, mutation of $EED^{67-69}$ or $YES^{70-72}$ affects the $LL^{76,77}$-based motif in a way that they do not affect the $LL^{76,77}$-based motif in the complete cytoplasmic domain. These complications notwithstanding, it is clear that the sequences between 55 and 84 contain information that promotes rapid internalization as well as slow recycling, from which we conclude that this region is necessary and sufficient for dynamic retention within endosomes.

### *Motif-mediated Retention of IRAP in the ERC*

Based on the morphological and fluorescence-quenching analyses presented here and previously, we propose a model in which vpTR is trafficked through the same compartment as the TR (Johnson *et al.*, 1998). In this model the differences in the kinetics of vpTR and TR trafficking reflect differences in the rate of transport from the ERC rather than differences in the targeting of TR and vpTR proteins to distinct recycling compartments. The observation that the rapidly recycled mutants of vpTR are also in the same intracellular compartment as the slowly recycled wild-type vpTR provides further support for this model. Thus, trafficking of vpTR in CHO cells provides a system for analysis of a kinetically distinct endocytic recycling mechanism.

Our finding that the rate of transport of IRAP from endosomes is determined by a motif that is of the same class of motifs that regulate concentration of proteins in transport vesicles provides a conceptual framework for understanding the retention mechanism. Three general classes of endocytic trafficking motifs have been identified: aromatic amino acid-based motifs, nonpolar amino acid-based motifs (e.g., di-leucine–based motifs), and motifs based on clusters of acidic amino acids (Keller and Simons, 1997; Traub and Kornfeld, 1997). These three classes of motifs are involved in internalization through clathrin-coated pits as well as targeted trafficking among membrane compartments. These motifs determine membrane protein trafficking by specifically linking cargo proteins to coat proteins that are involved in vesicle formation, thereby concentrating cargo in specific transport vesicles. The "adaptin" complex family is the best-characterized class of proteins that binds trafficking motifs (Schmid, 1997; Le and Hoflack, 1998; Scales *et al.*, 2000), although proteins that bind trafficking motifs have been identified that are not members of the adaptin family (e.g., Diaz and Pfeffer, 1998; Wan *et al.*, 1998; Krise *et al.*, 2000; Orsel *et al.*, 2000). In addition to adaptins linking cargo proteins to transport vesicles, there is evidence for a direct association between trafficking motifs and clathrin (Kibbey *et al.*, 1998).

By analogy to the role that the di-leucine and acidic cluster motifs play in other membrane protein transport processes, we propose a mechanism by which an adaptin-like protein binds the di-leucine/acidic cluster of IRAP. As a result of this binding IRAP (and its surrogate vpTR) is concentrated in transport vesicles that bud more slowly from the ERC than transport vesicles that mediate recycling of TR back to the cell surface. We propose that IRAP is excluded from the fast recycling pathway (i.e., that followed by the TR) by virtue of its efficient concentration in the slow transport vesicles. When the acidic cluster/di-leucine retention motif is mutated, IRAP is no longer concentrated in the slowly budding transport vesicles and is therefore returned to the surface by the rapidly budding TR-containing vesicles. The TR is rapidly transported from the ERC back to the cell surface by a non-motif–mediated mechanism (e.g., Mayor *et al.*, 1993). In our model for IRAP trafficking, the TR is not actively excluded from the IRAP-containing transport vesicles. However, because the TR can enter the rapidly budding recycling vesicles, it is more likely, based on the kinetics, that the TR will be recycled by the rapid pathway. The rate of budding of the slow transport vesicles is a potential site of regulation of IRAP's recycling, and therefore one possible explanation for the effect of insulin on the recycling of vpTR is that it stimulates the rate of budding of these vesicles.

An alternative model for the dynamic retention of IRAP is that the acidic cluster/di-leucine motif mediates a segregation of IRAP to specialized regions of the ERC that are unable to form transport vesicles. In this case, the slow recycling rate constant of vpTR would reflect inefficient retention, with the molecules that have escaped retention returning to the cell surface in the TR-containing recycling vesicles. Although we favor the former model, our data do not distinguish between these models.

There is considerable precedent for distinct transport vesicles budding from a single membrane compartment. For example, a number of functionally distinct vesicles bud from the TGN. The ERC may play a similar functional role in the endosomal system by serving as a sorting station of internalized proteins (e.g., Ghosh *et al.*, 1998; Mallet and Maxfield, 1999), as well as storage reservoir for the regulated recruitment of proteins to the plasma membrane. Consistent with this proposal, various coat and adaptin proteins have been localized to endosomes (Stoorvogel *et al.*, 1996; Stoorvogel, 1998), and recent evidence suggests that that rab proteins, regulators of membrane trafficking, are localized to distinct membrane "domains" of endosomal compartments (Sonnichsen *et al.*, 2000). This heterogeneity of endosomal membranes may reflect sites for the formation of distinct transport vesicles.

Acidic cluster/di-leucine motifs are involved in a number of distinct, specialized trafficking processes. Presumably these motifs bind to different adaptin proteins and thereby target proteins to specialized transport vesicles (Rohn *et al.*, 2000). Various di-leucine and acidic cluster/di-leucine motifs have been shown to bind to AP-1, AP-2, and AP-3 adaptins (Dietrich *et al.*, 1997; Honing *et al.*, 1998; Rapoport *et al.*, 1998; Heilker *et al.*, 1999). However, the molecular details that determine the specificity of binding of a given

acidic cluster/di-leucine motif to a specific adaptin complex are not known. Therefore, it is not fruitful at this time to speculate on which adaptin complex binds the IRAP acidic cluster/di-leucine motif based on the sequence of IRAP's trafficking motif.

### *Implications of IRAP Trafficking in Fibroblasts for Understanding Insulin-regulated Trafficking in Differentiated Cell Types*

IRAP is highly expressed in fat and muscle cells, where it is trafficked by the same specialized insulin-regulated mechanism as the GLUT4 glucose transporter (Ross *et al.*, 1996, 1997). The relationship between the insulin-regulated trafficking pathways in CHO cells and these differentiated cell types is not understood at this time; therefore, we cannot conclude that the motifs we have identified in studies of CHO cells determine IRAP trafficking in the differentiated cells. However, we have shown that vpTR expressed in 3T3-L1 adipocytes is a valid surrogate for IRAP trafficking in those cells, and that $LL^{76,77}$ is required for dynamic retention of vpTR in 3T3-L1 cells (Subtil *et al.*, 2000). Those findings are consistent with IRAP's trafficking motifs functioning in both adipocytes and CHO cells. In addition, we and others have shown that insulin stimulates a two- to threefold translocation of GLUT4 to the cell surface when it is expressed in CHO cells (Kanai *et al.*, 1993; Lampson *et al.*, 2000). Thus, the two proteins known to be transported by an insulin-regulated pathway in fat and muscle cells are also trafficked by an insulin-regulated pathway in CHO cells. These findings indicate similarities in the insulin-regulated pathways in fibroblasts and fat cells and thereby suggest that the motifs identified in our analysis of CHO cells are relevant to the trafficking of IRAP in adipocytes. Although it is important to note that in fat cells insulin-induced translocation of GLUT4 and IRAP to the cell surface is considerably larger (~5- to 10-fold increase in surface) than what we observe in CHO cells. It may be that GLUT4 and IRAP are sorted from the endosomal system to a specialized compartment in fat cells and that targeting to this specialized compartment underlies the more pronounced effect of insulin on the behavior of these proteins in fat cells. Studies of the behaviors of the vpTR mutant constructs expressed in 3T3-L1 adipocytes, which will address these questions, are underway.

The observation that IRAP and GLUT4 are the only proteins known to be trafficked by the insulin-regulated pathway suggests that the motifs that determine their trafficking are similar. Our finding that retention of vpTR is dependent on an acidic cluster/di-leucine motif is in agreement with the results that a di-leucine sequence and acidic residues in the carboxyl cytoplasmic domain of GLUT4 play a critical role in its specialized trafficking (Verhey *et al.*, 1995; Martinez-Arca *et al.*, 2000; Shewan *et al.*, 2000). It is important to note, however, that the spacing between the acidic cluster and di-leucine sequence is quite different in GLUT4 and IRAP. In addition, the mutagenesis is not at this time extensive enough to allow for a detailed comparison of the acidic clusters of GLUT4 and IRAP. Thus, although these similarities are provocative, additional studies are required to establish that similar motifs determine trafficking of IRAP and GLUT4. In this regard, it should be noted that there is controversy regarding the motifs that determine GLUT4 trafficking. In addition to the di-leucine and acidic cluster sequences on the carboxyl cytoplasmic domain, a phenylalanine-based motif on the amino-terminal cytoplasmic domain is also involved in trafficking (Garippa *et al.*, 1994; Marsh *et al.*, 1995a).

Regardless of the ultimate relationship between IRAP and GLUT4 trafficking motifs, or for that matter the exact relationship between the IRAP trafficking in fibroblasts and fat cells, our analysis establishes that a di-leucine and a cluster of acidic amino acids target vpTR to a novel recycling pathway that is kinetically distinct from the previously characterized general endosomal recycling pathway. It is likely that dynamic retention in endosomes is of general importance because it affords the cells a specific mechanism for the rapid and reversible regulation of the distribution of proteins between the interior and surface of cells

## ACKNOWLEDGMENTS

We thank Alona Cohen and Agathe Subtil for helpful comments and discussions. This work was supported by National Institutes of Health grant DK52852 and a research grant from Metabolex, Inc.

## REFERENCES

Andersson, H., Kappeler, F., and Hauri, H.-P. (1999). Protein targeting to endoplasmic reticulum by dilysine signals involves direct retention in addition to retrieval. J. Biol. Chem. *274*, 15080–15084.

Bryant, N.J., and Stevens, T.H. (1997). Two separate signals act independently to localize a yeast late Golgi membrane protein through a combination of retrieval and retention. J. Cell Biol. *136*, 287–297.

Collawn, J.F., Stangel, M., Kuhn, L.A., Esekogwu, V., Jing, S.Q., Trowbridge, I.S., and Tainer, J.A. (1990). Transferrin receptor internalization sequence YXRF implicates a tight turn as the structural recognition motif for endocytosis. Cell *63*, 1061–1072.

Cosson, P., Lefkir, Y., Demolliere, C., and Letourneur, F. (1998). New COP1-binding motifs involved in ER retrieval. EMBO J. *17*, 6863–6870.

Diaz, E., and Pfeffer, S. (1998). TIP47: a cargo selection device for mannose 6-phosphate receptor trafficking. Cell *93*, 433–443.

Dietrich, J., Kastrup, J., Nielsen, B., Odum, N., and Geisler, C. (1997). Regulation and function of the CD3gamma DxxxLL motif: a binding site for adaptor protein-1 and adaptor protein-2 in vitro. J. Cell Biol. *138*, 271–281.

Eng, F., Varlamov, O., and Fricker, L. (1999). Sequences within the cytoplasmic domain of gp180/carboxypeptidase D mediate localization to the trans-Golgi network. Mol. Biol. Cell *10*, 35–46.

Garippa, R.J., Judge, T.W., James, D.E., and McGraw, T.E. (1994). The amino terminus of GLUT4 functions as an internalization motif but not an intracellular retention signal when substituted for the transferrin receptor cytoplasmic domain. J. Cell Biol. *124*, 705–715.

Ghosh, R.N., Mallet, W.G., Soe, T.T., McGraw, T.E., and Maxfield, F.R. (1998). An endocytosed TGN38 chimeric protein is delivered to the TGN after trafficking through the endocytic recycling compartment in CHO cells. J. Cell Biol. *142*, 923–936.

Heilker, R., Spiess, M., and Crottet, P. (1999). Recognition of sorting signals by clathrin adaptors. Bioessays *21*, 558–567.

Honing, S., Sandoval, I.V., and von Figura, K. (1998). A di-leucine-based motif in the cytoplasmic tail of LIMP-II and tyrosinase mediates selective binding of AP-3. EMBO J. *17*, 1304–1314.

Jackson, M.R., Nilsson, T., and Peterson, P.A. (1990). Identification of a consensus motif for retention of transmembrane proteins in the endoplasmic reticulum. EMBO J. *9*, 3153–3162.

Jing, S.Q., Spencer, T., Miller, K., Hopkins, C., and Trowbridge, I.S. (1990). Role of the human transferrin receptor cytoplasmic domain in endocytosis: localization of a specific signal sequence for internalization. J. Cell Biol. *110*, 283–294.

Johnson, A.O., Subtil, A., Petrush, R., Kobylarz, K., Keller, S.R., and McGraw, T.E. (1998). Identification of an insulin-responsive, slow endocytic recycling mechanism in Chinese hamster ovary cells. J. Biol. Chem. *273*, 17968–17977.

Johnson, L.S., Dunn, K.W., Pytowski, B., and McGraw, T.E. (1993). Endosome acidification and receptor trafficking: bafilomycin A1 slows receptor externalization by a mechanism involving the receptor's internalization motif. Mol. Biol. Cell *4*, 1251–1266.

Jones, B.G., Thomas, L., Molloy, S.S., Thulin, C.D., Fry, M.D., Walsh, K.A., and Thomas, G. (1995). Intracellular trafficking of furin is modulated by the phosphorylation state of a casein kinase II site in its cytoplasmic tail. EMBO J. *14*, 5869–5883.

Kanai, F., Nishioka, Y., Hayashi, H., Kamohara, S., Todaka, M., and Ebina, Y. (1993). Direct demonstration of insulin-induced GLUT4 translocation to the surface of intact cells by insertion of a c-myc epitope into an exofacial GLUT4 domain. J. Biol. Chem. *268*, 14523–14526.

Kandror, K.V., and Pilch, P.F. (1994). gp160, a tissue-specific marker for insulin-activated glucose transport. Proc. Natl. Acad. Sci. USA *91*, 8017–8021.

Kandror, K.V., Yu, L., and Pilch, P.F. (1994). The major protein of GLUT4-containing vesicles, gp160, has aminopeptidase activity. J. Biol. Chem. *269*, 30777–30780.

Keller, P., and Simons, K. (1997). Post-Golgi biosynthetic trafficking. J. Cell Sci. *110*, p3001–3009.

Keller, P., and Simons, K. (1998). Cholesterol is required for surface transport of influenza virus hemagglutinin. J. Cell Biol. *140*, 1357–1367.

Keller, S.R., Scott, H.M., Mastick, C.C., Aebersold, R., and Lienhard, G.E. (1995). Cloning and characterization of a novel insulin-regulated membrane aminopeptidase from Glut4 vesicles. J. Biol. Chem. *270*, 23612–23618.

Kibbey, R., Rizo, J., Gierasch, L., and Anderson, R. (1998). The LDL receptor clustering motif interacts with the clathrin terminal domain in a reverse turn conformation. J. Cell Biol. *142*, 59–67.

Koval, M., and Pagano, R. (1989). Lipid recycling between the plasma membrane and intracellular compartments: transport and metabolism of fluorescent sphingomyelin analogues in cultured fibroblasts. J. Cell Biol. *108*, 2169–2181.

Koval, M., and Pagano, R. (1990). Sorting of an internalized plasma membrane lipid between recycling and degradative pathways in normal and Niemann-Pick, type A fibroblasts. J. Cell Biol. *111*, 429–442.

Krise, J., Sincock, P., Orsel, J., and Pfeffer, S. (2000). Quantitative analysis of TIP47-receptor cytoplasmic domain interactions: implications for endosome-to-trans Golgi network trafficking. J. Biol. Chem. *275*, 25188–25193.

Lampson, M.A., Racz, A., Cushman, S.W., and McGraw, T.E. (2000). Demonstration of insulin-responsive trafficking of GLUT4 and vpTR fibroblasts. J. Cell Sci. *113*, 4065–4076.

Le, B.R., and Hoflack, B. (1998). Mechanisms of protein sorting and coat assembly: insights from the clathrin-coated vesicle pathway. Curr. Opin. Cell Biol. *10*, 499–503.

Liu, G., Thomas, L., Warren, R.A., Enns, C.A., Cunningham, C.C., Hartwig, J.H., and Thomas, G. (1997). Cytoskeletal protein ABP-280 directs the intracellular trafficking of furin and modulates proprotein processing in the endocytic pathway. J. Cell Biol. *139*, 1719–1733.

Mallet, W.G., and Maxfield, F.R. (1999). Chimeric forms of furin and TGN38 are transported with the plasma membrane in the trans-Golgi network via distinct endosomal pathways. J. Cell Biol. *146*, 345–359.

Marsh, B.J., Alm, R.A., McIntosh, S.R., and James, D.E. (1995a). Molecular regulation of GLUT-4 targeting in 3T3–L1 adipocytes. J. Cell Biol. *130*, 1081–1091.

Marsh, E.W., Leopold, P.L., Jones, N.L., and Maxfield, F.R. (1995b). Oligomerized transferrin receptors are selectively retained by a lumenal sorting signal in a long-lived endocytic recycling compartment. J. Cell Biol. *129*, 1509–1522.

Martinez-Arca, S., Lalioti, V., and Sandoval, I. (2000). Intracellular targeting and retention of the glucose transporter GLUT4 by the perinuclear storage compartment involves distinct carboxyl-tail motifs. J. Cell Sci. *113*, 1705–1715.

Mayor, S., Presley, J.F., and Maxfield, F.R. (1993). Sorting of membrane components from endosomes and subsequent recycling to the cell surface occurs by a bulk flow process. J. Cell Biol. *121*, 1257–1269.

Mayor, S., Rothberg, K.G., and Maxfield, F.R. (1994). Sequestration of GPI-anchored proteins in caveolae triggered by cross-linking. Science *264*, 1948–1951.

Mayor, S., Sabharanjak, S., and Maxfield, F.R. (1998). Cholesterol-dependent retention of GPI-anchored proteins in endosomes. EMBO J. *17*, 4626–4638.

Mays, R.W., Siemers, K.A., Fritz, B.A., Lowe, A.W., van Meer, G., and Nelson, W.J. (1995). Hierarchy of mechanisms involved in generating Na/K-ATPase polarity in MDCK epithelial cells. J. Cell Biol. *130*, 1105–1115.

McGraw, T.E., Greenfield, L., and Maxfield, F.R. (1987). Functional expression of the human transferrin receptor cDNA in Chinese hamster ovary cells deficient in endogenous transferrin receptor. J. Cell Biol. *105*, 207–214.

Nilsson, T., Lucocq, J.M., Mackay, D., and Warren, G. (1991). The membrane spanning domain of beta-1,4-galactosyltransferase specifies trans Golgi localization. EMBO J. *10*, 3567–3575.

Orsel, J., Sincock, P., Krise, J., and Pfeffer, S. (2000). Recognition of the 300-kDa mannose 6-phosphate receptor cytoplasmic domain by 47-kDa tail-interacting protein. Proc. Natl. Acad. Sci. USA *97*, 9047–9051.

Presley, J.F., Mayor, S., McGraw, T.E., Dunn, K.W., and Maxfield, F.R. (1997). Bafilomycin A1 treatment retards transferrin receptor recycling more than bulk membrane recycling. J. Biol. Chem. *272*, 13929–13936.

Rapoport, I., Chen, Y.C., Cupers, P., Shoelson, S.E., and Kirchhausen, T. (1998). Dileucine-based sorting signals bind to the beta chain of AP-1 at a site distinct and regulated differently from the tyrosine-based motif-binding site. EMBO J. *17*, 2148–2155.

Raub, T.J., Koroly, M.J., and Roberts, R.M. (1990). Endocytosis of wheat germ agglutinin binding sites from the cell surface into a tubular endosomal network. J. Cell. Physiol. *143*, 1–12.

Rohn, W., Rouille, Y., Waguri, S., and Hoflack, B. (2000). Bi-directional trafficking between the trans-Golgi network and the endosomal/lysosomal system. [record supplied by publisher] J. Cell Sci. *113*, 2093–2101.

Ross, S.A., Herbst, J.J., Keller, S.R., and Lienhard, G.E. (1997). Trafficking kinetics of the insulin-regulated membrane aminopeptidase in 3T3–L1 adipocytes. Biochem. Biophys. Res. Commun. *239*, 247–251.

Ross, S.A., Scott, H.M., Morris, N.J., Leung, W.Y., Mao, F., Lienhard, G.E., and Keller, S.R. (1996). Characterization of the insulin-regulated membrane aminopeptidase in 3T3–L1 adipocytes. J. Biol. Chem. *271*, 3328–3332.

Rothman, J.E., and Wieland, F.T. (1996). Protein sorting by transport vesicles. Science *272*, 227–234.

Scales, S., Gomez, M., and Kreis, T. (2000). Coat proteins regulating membrane traffic. Int. Rev. Cytol. *195*, 67–144.

Schafer, W., Stroh, A., Berghofer, S., Seiler, J., Vey, M., Kruse, M.L., Kern, H.F., Klenk, H.D., and Garten, W. (1995). Two independent targeting signals in the cytoplasmic domain determine trans-Golgi network localization and endosomal trafficking of the proprotein convertase furin. EMBO J. *14*, 2424–2435.

Schmid, S. (1997). Clathrin-coated vesicle formation and protein sorting: an integrated process. Annu. Rev. Biochem. *66*, 511–548.

Shewan, A.M., Marsh, B.J., Melvin, D.R., Martin, S., Gould, G.W., and James, D.E. 2000. The cytosolic c-terminus of the glucose transporter GLUT4 contains acidc cluster endosomal targeting motif distal to the dileucine signal. Biochem. J. *350*, 99–107.

Simons, K., and Ikonen, E. (1997). Functional rafts in cell membranes. Nature *387*, 569–572.

Sonnichsen, B., De, R.S., Nielsen, E., Rietdorf, J., and Zerial, M. (2000). Distinct membrane domains on endosomes in the recycling pathway visualized by multicolor imaging of Rab4, Rab5, and Rab11. J. Cell Biol. *149*, 901–914.

Stoorvogel, W. (1998). Analysis of the endocytic system by using horseradish peroxidase. Trends Cell Biol. *8*, 503–505.

Stoorvogel, W., Oorschot, V., and Geuze, H. (1996). A novel class of clathrin-coated vesicles budding from endosomes. J. Cell Biol. *132*, 21–33.

Subtil, A., Lampson, M., Keller, S., and McGraw, T. (2000). Characterization of the insulin-regulated endocytic recycling mechanism in 3T3–L1 adipocytes using a novel reporter molecule. J. Biol. Chem. *275*, 4787–4795.

Sutterlin, C., Doering, T.L., Schimmoller, F., Schroder, S., and Riezman, H. (1997). Specific requirements for the ER to Golgi transport of GPI-anchored proteins in yeast. J. Cell Sci. *110*, 2703–2714.

Swift, A.M., and Machamer, C.E. (1991). A Golgi retention signal in a membrane-spanning domain of coronavirus E1 protein. J. Cell Biol. *115*, 19–30.

Takahashi, S., Nakagawa, T., Banno, T., Watanabe, T., Murakami, K., and Nakayama, K. (1995). Localization of furin to the trans-Golgi network and recycling from the cell surface involves Ser and Tyr residues within the cytoplasmic domain. J. Biol. Chem. *270*, 28397–28401.

Traub, L., and Kornfeld, S. (1997). The trans-Golgi network: a late secretory sorting station. Curr. Opin. Cell Biol. *9*, 527–533.

Trowbridge, I.S., Collawn, J.F., and Hopkins, C.R. (1993). Signal-dependent membrane protein trafficking in the endocytic pathway. Annu. Rev. Cell Biol. *9*, 129–161.

Verhey, K.J., Yeh, J.I., and Birnbaum, M.J. (1995). Distinct signals in the GLUT4 glucose transporter for internalization and for targeting to an insulin-responsive compartment. J. Cell Biol. *130*, 1071–1079.

Wan, L., Molloy, S.S., Thomas, L., Liu, G., Xiang, Y., Rybak, S.L., and Thomas, G. (1998). PACS-1 defines a novel gene family of cytosolic sorting proteins required for trans-Golgi network localization. Cell *94*, 205–216.

Xiang, Y., Molloy, S., Thomas, L., and Thomas, G. (2000). The PC6B cytoplasmic domain contains two acidic clusters that direct sorting to distinct trans-Golgi network/endosomal compartments. Mol. Biol. Cell *11*, 1257–1273.

Yamashiro, D.J., Tycko, B., Fluss, S.R., and Maxfield, F.R. (1984). Segregation of transferrin to a mildly acidic (pH 6.5) para-Golgi compartment in the recycling pathway. Cell *37*, 789–800.